Kv4 potassium channels modulate hippocampal EPSP-spike potentiation and spatial memory in rats

Bruno Truchet, Christine Manrique, Leam Sreng, Franck A Chaillan, Francois S. Roman, Christianne Mourre

Kv4 potassium channels modulate hippocampal EPSP-spike potentiation and spatial memory in rats

Bruno Truchet, Christine Manrique, Leam Sreng, et al.

Learn. Mem. 2012 19: 282-293
Access the most recent version at doi:10.1101/lm.025411.111

Research

Kv4 potassium channels modulate hippocampal EPSP-spike potentiation and spatial memory in rats

Bruno Truchet,[1] Christine Manrique,[2] Leam Sreng,[3] Franck A. Chaillan,[1] François S. Roman,[4] and Christiane Mourre[1,5]

[1]*Laboratory of Neuroscience and Cognition (LNC-UMR 7291), Centre National de la Recherche Scientifique—Aix-Marseille Université, Centre Saint-Charles, 13331 Marseille, France;* [2]*Fédération de Recherche (Comportement-Cerveau-Cognition) (3C-FR 3512), Centre National de la Recherche Scientifique—Aix-Marseille Université, Centre Saint-Charles, 13331 Marseille, France;* [3]*Laboratoire Evolution, Génome, Environnement (EGE-UMR 7263), Centre National de la Recherche Scientifique-Aix-Marseille Université, IMBE, Centre Saint-Charles, 13331 Marseille, France;* [4]*Laboratoire de Neurobiologie des interactions cellulaires et neurophysiopathologie (NICN-UMR7259), Centre National de la Recherche Scientifique—Aix-Marseille Université, Faculté de Médecine Nord, 13344 Marseille, France*

Kv4 channels regulate the backpropagation of action potentials (b-AP) and have been implicated in the modulation of long-term potentiation (LTP). Here we showed that blockade of Kv4 channels by the scorpion toxin AmmTX3 impaired reference memory in a radial maze task. In vivo, AmmTX3 intracerebroventricular (i.c.v.) infusion increased and stabilized the EPSP-spike (E-S) component of LTP in the dentate gyrus (DG), with no effect on basal transmission or short-term plasticity. This increase in E-S potentiation duration could result from the combination of an increase in excitability of DG granular cells with a reduction of GABAergic inhibition, leading to a strong reduction of input specificity. Radioactive in situ hybridization (ISH) was used to evaluate the amounts of Kv4.2 and Kv4.3 mRNA in brain structures at different stages of a spatial learning task in naive, pseudoconditioned, and conditioned rats. Significant differences in Kv4.2 and Kv4.3 mRNA levels were observed between conditioned and pseudoconditioned rats. Kv4.2 and Kv4.3 mRNA levels were transiently up-regulated in the striatum, nucleus accumbens, retrosplenial, and cingulate cortices during early stages of learning, suggesting an involvement in the switch from egocentric to allocentric strategies. Spatial learning performance was positively correlated with the levels of Kv4.2 and Kv4.3 mRNAs in several of these brain structures. Altogether our findings suggest that Kv4 channels could increase the signal-to-noise ratio during information acquisition, thereby allowing a better encoding of the memory trace.

[Supplemental material is available for this article.]

Regulation of ion-channel activity is involved in strengthening of synaptic connections during information processing. Among the potassium channels that are key to neuronal excitability, A-type potassium channels are important regulators of signal integration and propagation in dendrites. Neuromodulators strongly regulate these channels through phosphorylation, association with auxiliary subunits, and expression-level control. A-type potassium channels modulate the action potential broadening, b-AP (backpropagation of action potentials), spike generation, and integration of synaptic inputs (Ramakers and Storm 2002; Watanabe et al. 2002; Yuan et al. 2002; Birnbaum et al. 2004; Lauver et al. 2006; Hammond et al. 2008; Kim and Hoffman 2008). Among the A-type potassium channels, the Kv4 channels adjust dendritic function by limiting spike-timing-dependent plasticity. This mode of action requires the co-occurrence of an EPSP and a b-AP (Magee and Johnston 1997, 2005; Birnbaum et al. 2004; Zhao et al. 2011).

There are several lines of evidence suggesting that Kv4 channels may play a role in learning and memory. Indeed, deletion of the Kv4.2 gene facilitates the induction of long-term potentiation (LTP) in CA1, a hippocampal field involved in mnesic processes (Chen et al. 2006). Besides, in hippocampal neuron cultures, Kv4.2 mRNA levels are up-regulated following depolarization in a NMDA receptor and Ca^{2+}-dependent fashion (Jo and Kim 2011). In fact, a bidirectional expression regulation of the Kv4.2 channel was found in the hippocampus within the dynamic range of synaptic plasticity. NMDA receptor activation not only transiently reduces Kv4.2 protein level due to degradation, but also increases Kv4.2 protein production in a fragile × mental retardation protein-dependent process likely involving Kv4.2-3′UTR (Lei et al. 2010; Lee et al. 2011). Furthermore, deficits in spatial memory and context discrimination are associated with a reduction of Kv4.2 channel phosphorylation (Morozov et al. 2003), whereas reduction in surface expression of Kv4.2 channels parallels impairments in spatial memory in status epilepticus (Lugo et al. 2008; Monaghan et al. 2008). Recently, Lockridge and Yuan (2011) showed that Kv4.2 knockout mice are impaired in a spatial learning task.

The use of specific blockers of Kv4 channels is a powerful tool to investigate their functions in vivo. Recently, three "short-chain" scorpion toxins, Aa1 from *Androctonus australis,* BmTX3 from *Buthus martensi,* and AmmTX3 from *Androctonus mauretanicus* (Pisciotta et al. 2000; Vacher et al. 2001, 2004) have been described as specific blockers of Kv4 channels. Binding and displacement experiments using rat brain synaptosomes showed that AmmTX3 and Aa1 competed effectively with 125 I-labeled

[5]Corresponding author
E-mail christiane.mourre@univ-amu.fr
Article is online at http://www.learnmem.org/cgi/doi/10.1101/lm.025411.111.

sBmTX3 binding. They fully inhibited the 125 I-labeled sBmTX3 binding (Ki values of 19.5 pM and 44.2 pM, respectively), demonstrating unambiguously that the three molecules shared the same target in rat brain (Vacher et al. 2002). BmTX3 inhibits the A-type current of Kv4.1-3 transfected into COS-7 cells (Vacher et al. 2006). Furthermore, in many areas of the brain, there is an overlap in the distribution of BmTX3 binding sites and the Kv4 subunits. In the hippocampal formation, only the combined distributions of Kv4.2 and Kv4.3 subunits are identical to those of the BmTX3 binding sites (Sheng et al. 1992; Maletic-Savatic et al. 1995; Serôdio et al. 1996; Tsaur et al. 1997; Serôdio and Rudy 1998; Varga et al. 2000; Rhodes et al. 2004; Jinno et al. 2005; Menegola and Trimmer 2006; Vacher et al. 2006). Finally, Kv4.2 and Kv4.3 are highly expressed in the hippocampal dentate gyrus (DG) (Tsaur et al. 1997; Serôdio and Rudy 1998; Jinno et al. 2005), a key structure to perform a radial maze task (Sutherland et al. 1983; Jeltsch et al. 2001).

To investigate the role of Kv4 channels in learning and memory, we tested the effects of AmmTX3 on a radial maze spatial task and DG LTP in vivo and analyzed the variations in Kv4 subunit expression across learning sessions. Our results showed that AmmTX3 allowed the EPSP-spike (E-S) component of LTP, i.e., E-S potentiation, to last longer in DG through an increase in excitability probably combined with a reduction of GABAergic inhibition. This increase of E-S potentiation would lead to a strong reduction of input specificity resulting in an impairment of spatial memory. Moreover, a correlation between up-regulation of Kv4.2 and Kv4.3 mRNA and rat spatial performances was found in the striatum and limbic regions involved in strategy choice during the early stages of learning. These results suggest that Kv4 channels play a key role in the regulation of network plasticity during memory processes.

Results

Electrophysiology

Effect of AmmTX3 injection on basal transmission was assessed through baseline recording, Input-output (IO) curves, and on short-term plasticity through measurements of paired-pulse ratio (PPR). No difference was found between groups regarding all three parameters (see Supplemental Material for details and figures).

Long–term potentiation (Fig. 1)

Field EPSP (fEPSP) slope (Fig. 1A). We used a high-frequency stimulation (HFS) protocol in which the parameters were chosen to induce a moderate level of LTP. The average level of slope increase was low (AmmTX3: $16.1 \pm 10.8\%$; Vehicle: $12.9 \pm 7.5\%$). Slope remained above baseline for 30 min following HFS (AmmTX3: $F_{(1,12)} = 5.01$, $P < 0.05$; Vehicle: $F_{(1,10)} = 29.02$, $P < 0.001$). No difference was observed between AmmTX3 and vehicle groups at any post-HFS period considered ($F_{(1,11)} \leq 1.00$, NS).

Population spike (PS) amplitude (Fig. 1B). PS amplitude remained above baseline for the whole 4 h following HFS in both groups (AmmTX3: $F_{(1,12)} > 25.75$, $P < 0.001$; Vehicle: $F_{(1,10)} > 6.19$, $P < 0.05$). Between-group comparison showed no significant effect of AmmTX3 when considering the whole 4 h of LTP maintenance ($F_{(1,11)} = 2.30$, NS). However, while the PS amplitude decreased steadily in the vehicle group, this parameter remained stable across the recording in the AmmTX3 group. Indeed, a clear difference between the two groups developed across the maintenance phase, beginning 90 min post-induction ($F_{(1,11)} = 4.96$, $P < 0.05$).

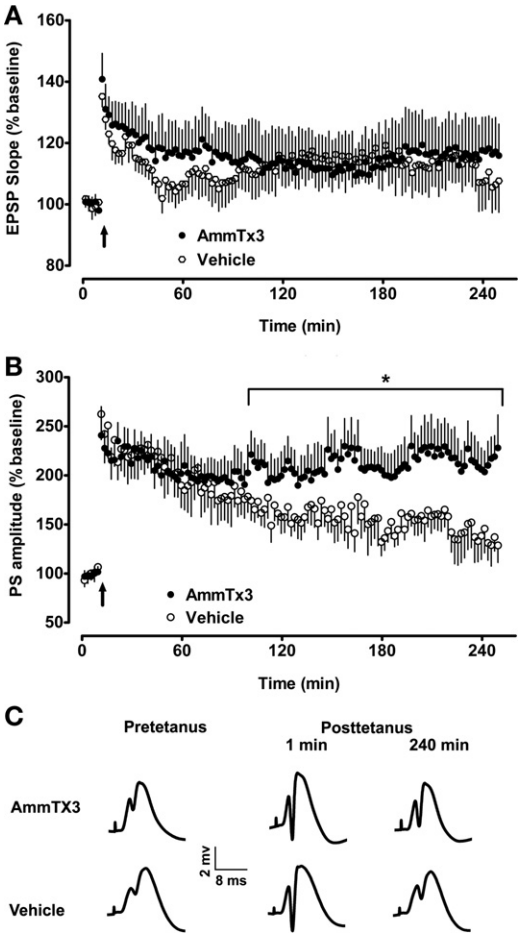

Figure 1. Effect of AmmTX3 on long-term potentiation. (*A*) Percentage changes of fEPSP slope. (*B*) Percentage changes of population spike (PS) amplitude. Dentate gyrus (DG) recording obtained before (10 min baseline) and after (4 h) a weak tetanus (arrow) of the MPP. (*A*,*B*) Data are expressed as mean ± SEM, $n = 7$ for AmmTX3 group, $n = 6$ for vehicle group. For clarity, each point represents the mean of four plotted measures. Data were normalized with respect to baseline level. (*C*) Representative traces of potential evoked in the DG by stimulation of the MPP, pre-tetanus (baseline) and post-tetanus, in both groups.

In conclusion, within-group analysis showed that the fEPSP component of LTP disappeared 30 min after induction, while the PS amplitude remained above baseline in both groups, which is characteristic of an EPSP-spike potentiation (E-S potentiation) (Bliss and Lomo 1973; Abraham et al. 1987). The main finding of our electrophysiological study is that AmmTX3 increases and stabilizes E-S potentiation from 90 min post-induction.

Effect of AmmTX3 on radial maze performance

Rats were subjected to a radial eight-arm maze task in which only three arms were baited.

Effect of AmmTX3 on radial–arm maze acquisition of spatial information (Table 1)

To analyze the effects on acquisition of spatial information, AmmTX3 and vehicle were injected 30 min before session 2. Table 1 shows that the AmmTX3 and vehicle groups improved their performance across sessions ($F_{(3,48)} = 21.56$, $P < 0.0001$). For the first session, (i.e., before the injection), ANOVA of reference

Table 1. Effects of AmmTX3 in spatial memory in an eight-arm radial task

Sessions	1	2	3	4	5	6
Reference memory errors						
Effects on acquisition						
Ammtx3 injection before Session 2						
Vehicle group	4.6 ± 0.05	3.38 ± 0.34	2.67 ± 0.47	1.58 ± 0.29	1.08 ± 0.24	
Ammtx3 group	4.07 ± 0.29	3.40 ± 0.21	2.60 ± 0.49	1.52 ± 0.18	1.15 ± 0.21	
Effects on consolidation						
Ammtx3 injection after session 3						
Vehicle group	4.33 ± 0.24	3.66 ± 0.26	3.22 ± 0.20	1.75 ± 0.13	1.79 ± 0.22	
Ammtx3 group	3.81 ± 0.27	3.44 ± 0.15	3.09 ± 0.27	2.47* ± 0.20	1.55 ± 0.13	
Ammtx3 injection after session 5						
Vehicle group	3.95 ± 0.30	3.18 ± 0.28	2.27 ± 0.33	1.40 ± 0.20	1.12 ± 0.28	0.80 ± 0.21
Ammtx3 group	4.29 ± 0.18	3.15 ± 0.17	2.44 ± 0.19	1.36 ± 0.17	0.91 ± 0.13	0.68 ± 0.13
Working memory errors						
Effects on acquisition						
Ammtx3 injection before session 2						
Vehicle group	1.40 ± 0.20	1.02 ± 0.26	1.02 ± 0.34	0.67 ± 0.15	0.44 ± 0.08	
Ammtx3 group	1.20 ± 0.34	0.93 ± 0.23	1.12 ± 0.36	0.48 ± 0.15	0.70 ± 0.20	
Effects on consolidation						
Ammtx3 injection after session 3						
Vehicle group	0.75 ± 0.21	0.94 ± 0.25	0.58 ± 0.19	0.64 ± 0.17	0.62 ± 0.18	
Ammtx3 group	0.81 ± 0.20	0.81 ± 0.18	0.72 ± 0.18	0.48 ± 0.17	0.34 ± 0.09	
Ammtx3 injection after session 5						
Vehicle group	0.63 ± 0.16	0.46 ± 0.15	0.35 ± 0.15	0.12 ± 0.04	0.17 ± 0.08	0.15 ± 0.09
Ammtx3 group	0.53 ± 0.16	0.31 ± 0.10	0.36 ± 0.14	0.23 ± 0.11	0.17 ± 0.08	0.21 ± 0.12

AmmTX3 (0.75 μg) was injected i.c.v. Mean numbers (±SEM) of memory errors in one daily session of six training trials, with a 2-min interval between trials, over 5 d. (Vehicle group) Injection before J2, $n = 8$; injection after J3, $n = 8$; injection after J5, $n = 10$; (AmmTX3 group) injection before J2, $n = 10$; injection after J3, $n = 11$; injection after J5, $n = 11$. (*) $P < 0.05$ in ANOVA comparing the vehicle group.

and working errors for the two groups indicated no difference ($F_{(1,16)} \leq 2.75$, NS). Following injection before session 2, working and reference errors were similar for the AmmTX3 and vehicle groups, and MANOVA indicated no interactions between group × session over the last four sessions ($F_{(3,48)} \leq 0.37$, NS). The number of both types of errors was similar for the AmmTX3 and vehicle groups over the three last sessions ($F_{(1,16)} \leq 1.55$, NS). In short, AmmTX3 did not impede normal acquisition.

Effect of AmmTX3 on radial–arm maze consolidation of spatial information

Reference memory errors (Table 1; Fig. 2). To analyze the effects on long-term consolidation of information at different stages of training, AmmTX3 and vehicle were injected immediately after sessions 1, 3, or 5. Distinct groups of rats were used for each injection time. The performances at injection time during these sessions were respectively weak, middle, and high, indicating that the mnesic trace became more consolidated across sessions. The AmmTX3 and vehicle groups improved their performance across sessions regardless of the injection time (ANOVA, $F_{(4,45)} \geq 21.56$, $P < 0.001$).

AmmTX3 injection after session 1. MANOVA showed that when injection was performed immediately after session 1, a significant group effect for reference errors was observed ($F_{(1,18)} = 8.71$, $P < 0.01$). This difference was due to the results from sessions 2 and 3 (ANOVA, $F_{(1,18)} \geq 6.18$, $P < 0.05$). Indeed, injection with AmmTX3 after session 1 impaired reference performance for at least two successive days (Fig. 2A). The comparison of reference memory errors between session 1 (before AmmTX3 injection) and session 2 (after AmmTX3 injection) indicated that both groups learned differently because a significant variation was found for vehicle group ($F_{(1,18)} = 13.27$, $P < 0.01$) and not for AmmTX3 group ($F_{(1,18)} = 4.01$, NS). In contrast, the variation of reference memory errors within each group between session 2

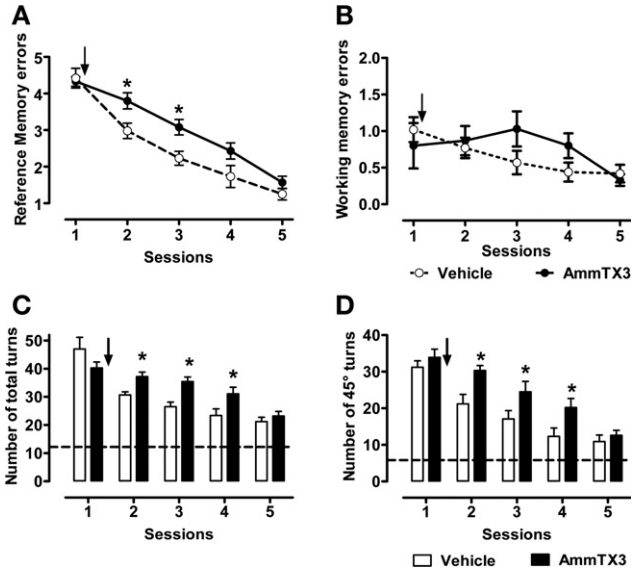

Figure 2. Spatial memory in an eight-arm radial task. I.c.v. injection was performed immediately after the first session (arrow). (*A*,*B*) Reference (*A*) and working (*B*) memory performances of vehicle ($n = 10$) and AmmTX3 ($n = 10$) groups. Mean numbers of memory errors during six training trials, constituting one daily session, with a 2-min interval between trials, over 5 d. Data are expressed as mean ± SEM. (*C*,*D*) Numbers of total turns (*C*) and 45° turns (*D*). Numbers of turns are means of six-trial sessions ± SEM. The dotted lines correspond to the maximal number of total turns (*A*) or 45° turns (*B*) when a rat performed without error during a session of six trials. (*) $P < 0.05$ in ANOVA comparing the vehicle and AmmTX3 groups.

and session 3 was significant ($F_{(1,18)} \geq 5.43$, $P < 0.05$) and similar for both groups ($F_{(1,18)} = 0.027$, NS) (Vehicle group: −25%; AmmTX3 group: −19%).

To assess the level of the gap between groups in the evolution of performance, we performed a between-group analysis for session n and session $n-1$. No significant performance difference was observed between AmmTX3 group on session 3 and vehicle group on session 2, or between AmmTX3 group on session 4 and vehicle group on session 3 ($F_{(1,18)} \leq 2.61$, NS). This means that learning was delayed by 1 d following AmmTX3 injection after session 1.

AmmTX3 injection after session 3. The injection of AmmTX3 after session 3 significantly increased the number of reference memory errors during session 4, in comparison to the vehicle group ($F_{(1,13)} = 5.70$, $P < 0.05$) (Table 1). However, no significant difference was observed in session 5 ($F_{(1,13)} = 2.74$, NS).

AmmTX3 injection after session 5. When injection of AmmTX3 was performed after session 5, the performances of both groups were similar during session 6 (ANOVAs, $F_{(1,19)} \leq 0.26$, NS) (Table 1).

Working memory errors (Table 1; Fig. 2B). Working memory performance was similar across sessions in all vehicle and AmmTX3 groups, regardless of the injection time, (ANOVAs, $F_{(1,18)} \leq 0.575$, NS). AmmTX3 did not affect working memory.

Analysis of the spatial strategy (Fig. 2C,D). Because only the rats injected after session 1 were seriously impaired, we conducted an analysis of the strategy used to solve the task only for this group and its control.

In Figure 2, C and D, dashed lines represent the theoretical number of turns done by a rat performing the task perfectly, i.e., without error in a session of six trials: 12 total turns and six 45° turns. Before injection, both groups, AmmTX3 and vehicle, performed similarly (ANOVAs, $F_{(1,18)} \leq 0.91$, NS). In both groups, the number of 45° and total turns decreased over the sessions, tending toward the dashed line. However, after injection of AmmTX3 immediately after session 1, the number of 45° and total turns was significantly higher compared with the vehicle group. ANOVAs showed an effect of toxin injection in sessions 2, 3, and 4 ($F_{(1,18)} \geq 4.35$, $P < 0.05$) for total turns and 45° turns, but not in session 5 ($F_{(1,18)} \leq 0.78$, NS).

In situ hybridization experiments (Table 2; Figs. 3–7)

Acquisition of spatial learning

In order to visualize Kv4 mRNA expression during learning, we trained different groups of rats in the eight-arm radial maze task and sacrificed them at different time points, i.e., after sessions 1, 2, 3, and 5. The number of reference memory errors decreased over the five sessions (Table 2; see Materials and Methods). MANOVA showed that reference memory improved between sessions, as shown by the significant decrease of errors ($F_{(4,69)} = 59.95$, $P < 0.001$). Similarly, the number of working memory errors decreased after session 2, reaching a mean of 0.3 working memory errors for session 5 ($F_{(4,69)} = 4.373$, $P < 0.01$) (Table 2).

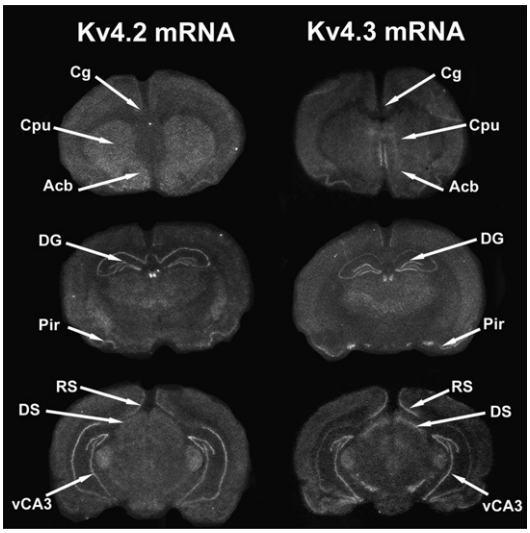

Figure 3. Kv4 mRNA ISH. Representative distributions of Kv4.2 mRNA and Kv4.3 mRNA in the forebrain and striatum (*top*), dorsal (*middle*), and ventral (*bottom*) hippocampus of naive rats. Kv4 mRNA signals were revealed by autoradiographic ISH using a specific antisense probe labeled with [^{35}S]. Brain regions were defined according to Paxinos and Watson (2007). White pixels represent a high level of mRNA labeling, and black pixels represent no labeling. (Acb) Nucleus accumbens; (CA3) ventral CA3 field; (Cg) cingulate cortex; (Cpu) striatum; (DS) dorsal subiculum; (Pir) piriform cortex; (RS) retrosplenial cortex.

Kv4 mRNA in situ hybridization

ISH experiments were performed to compare Kv4 expression in different groups at a given time (comparison of mRNA levels between the groups) and to examine the temporal evolution of Kv4 mRNA expression in a given experimental group (comparison of mRNA levels within a given group).

Figure 3 shows examples of the specific ISH signal patterns observed in the striatum, dorsal, and ventral hippocampal formation. Kv4.2 mRNA labeling was higher than Kv4.3 mRNA in the striatum. In the hippocampus, Kv4.2 mRNA content was high in all fields and the DG, whereas Kv4.3 mRNA was localized to the DG and CA3 field only. No significant differences were observed between the dorsal and ventral hippocampus. Furthermore, Kv4.3 mRNA labeling was particularly intense in the substantia nigra, pars compacta. Other learning-related neuronal structures including the habenula, cingulate cortex, and piriform cortex showed a moderate to high content of Kv4 mRNA. The overall distribution of Kv4 mRNA was similar to previous reports. High levels of Kv4.2 mRNA were found in the whole hippocampus, striatum, geniculate nuclei, and cerebellum, and high levels of Kv4.3 mRNA in the DG, CA3 field, retrosplenial cortex, geniculate nuclei, substantia nigra, and cerebellum (Serôdio et al. 1996; Tsaur et al. 1997; Martina et al. 1998; Serôdio and Rudy 1998; Rhodes et al. 2004).

In a between-group comparative analysis, for all times of sacrifice sections including 16 brain regions were subjected to hybridization in the same experiment and autoradiographed on an

Table 2. Spatial memory in an eight-arm radial task: in situ hybridization experiments

	Sessions				
	1	2	3	4	5
Reference errors	4.30 ± 0.20	2.80 ± 0.10	1.80 ± 0.40	0.60 ± 0.50	0.30 ± 0.030
Working errors	1.13 ± 0.29	1.11 ± 0.21	0.70 ± 0.26	0.60 ± 0.30	0.30 ± 0.020

Mean numbers of memory errors (±SEM) one daily session of six training trials, with a 2-min interval between trials, over 5 d. At each sacrifice time, conditioned group, $n = 6$. Reference and working memory performance of all rat groups sacrificed at different learning stages.

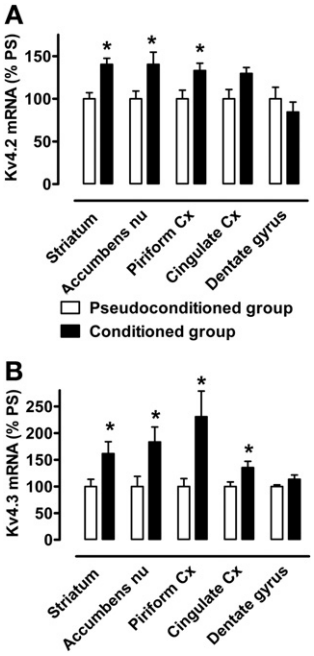

Figure 4. Kv4 mRNA ISH analysis. Kv4.2 (*A*) and Kv4.3 (*B*) mRNA levels for different structures in conditioned and pseudoconditioned rats sacrificed 1 h after session 1. Data are expressed as mean ± SEM of percentage of the mean value for the pseudoconditioned group. (*) $P < 0.05$ in ANOVA comparing pseudoconditioned (Kv4.2, $n = 6$; Kv4.3, $n = 6$) and conditioned (Kv4.2, $n = 5$; Kv4.3, $n = 5$) groups.

identical film sheet. These structures belong to the restricted and extended limbic system, and are implicated in learning and memory processes. They include the subiculum, habenula, striatum, nucleus accumbens, cortex (cingulate, retrosplenial, piriform, frontal), and the dorsal and ventral hippocampus (CA1, CA2, and CA3 fields and DG). The time course for changes in the level of Kv4 mRNA was analyzed for each pseudoconditioned and conditioned group (i.e., within-group temporal analysis).

For the naive and pseudoconditioned groups, levels of Kv4 mRNAs were found to be similar in all of the structures studied, regardless of the task session or time of sacrifice (ANOVA, $F_{(1,10)} \leq 4.49$, NS; data not shown).

Comparison of Kv4.2 mRNA levels between the conditioned and pseudoconditioned groups

Overall, the conditioned group appeared to have a transient increase in Kv4.2 mRNA expression in the basal ganglia and cortices (cingulate, piriform, retrosplenial) that was related to learning. In the hippocampal formation, only the ventral part of CA3 and subiculum was up-regulated in the conditioned group. In the other structures studied, there were no significant between-group differences in Kv4.2 mRNA levels at any of the learning stages.

One hour after session 1 (Fig. 4A). ANOVAs showed that the level of ISH labeling of Kv4.2 mRNA was higher in the conditioned group in the following brain structures: striatum, nucleus accumbens, and piriform cortex (+30%, $F_{(1,9)} \geq 5.51$, $P < 0.05$).

One hour after session 2 (Fig. 5A,B). Kv4.2 mRNA remained higher in the conditioned group in the striatum, nucleus accumbens, and piriform cortex (+50%, +85%, +50%, respectively, $F_{(1,9)} \geq 5.65$, $P < 0.05$). Expression of Kv4.2 mRNA in the conditioned group was also higher in the CA3 field of the hippocampus, the subiculum, and the retrosplenial cortex (+40%, $F_{(1,9)} \geq 6.67$, $P < 0.05$).

One hour after sessions 3 and 5. In all of the structures that were studied, ANOVAs indicated that there was no significant difference in Kv4.2 mRNA expression between groups ($F_{(1,9)} \leq 3.31$, NS, data not shown).

Comparison of Kv4.3 mRNA levels between the conditioned and pseudoconditioned groups

As with Kv4.2 mRNA, the expression of Kv4.3 mRNA appeared to undergo a transient increase in the basal ganglia and some of the cortices (piriform, cingulate) in the conditioned group of rats during the spatial learning task. However, in contrast to Kv4.2 mRNA, there was no change in the expression of Kv4.3 mRNA in the hippocampal formation ($F_{(1,9)} \leq 1.75$, NS).

One hour after session 1 (Fig. 4B). The level of Kv4.3 mRNA was higher in conditioned rats in the following brain structures: striatum, nucleus accumbens, and piriform cortex (+60%, +80%, +130%, respectively, $F_{(1,9)} \geq 5.49$, $P < 0.05$). Conditioned rats also showed higher levels of Kv4.3 mRNA in the cingulate cortex (+36%, $F_{(1,9)} = 5.63$, $P < 0.05$).

One hour after session 2 (Fig. 5C,D). The level of Kv4.3 mRNA in the striatum, nucleus accumbens, and piriform cortex was markedly higher in conditioned rats (+165%, +124%, +63%, respectively, $F_{(1,9)} \geq 6.03$, $P < 0.05$). In contrast to Kv4.2 mRNA, both groups showed similar levels of Kv4.3 mRNA in the CA3 field, subiculum, and retrosplenial cortex ($F_{(1,9)} \leq 1.76$, NS).

One hour after sessions 3 and 5. Conditioned and pseudoconditioned rats showed no differences in Kv4.3 mRNA levels in any of the brain structures studied ($F_{(1,9)} \leq 0.70$, NS, data not shown).

Temporal analysis (Fig. 6)

The purpose of this analysis was to identify any variation in the expression of Kv4 mRNA within a given brain structure during a

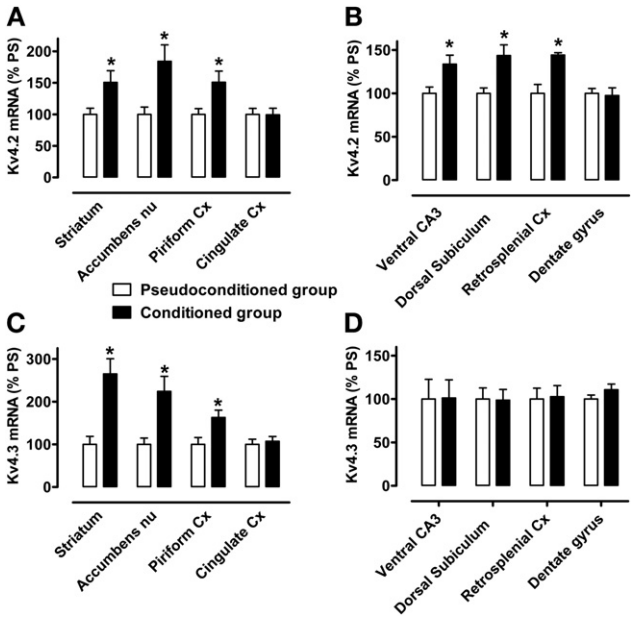

Figure 5. Kv4 mRNA ISH analysis. Kv4.2 (*A,B*) and Kv4.3 (*C,D*) mRNA levels in different structures for conditioned and pseudoconditioned rats sacrificed 1 h after session 2. Data are expressed as mean ± SEM of percentage of mean value for the pseudoconditioned group. (*) $P < 0.05$ in ANOVA, comparing pseudoconditioned (Kv4.2, $n = 6$; Kv4.3, $n = 6$) and conditioned (Kv4.2, $n = 5$; Kv4.3, $n = 5$) groups.

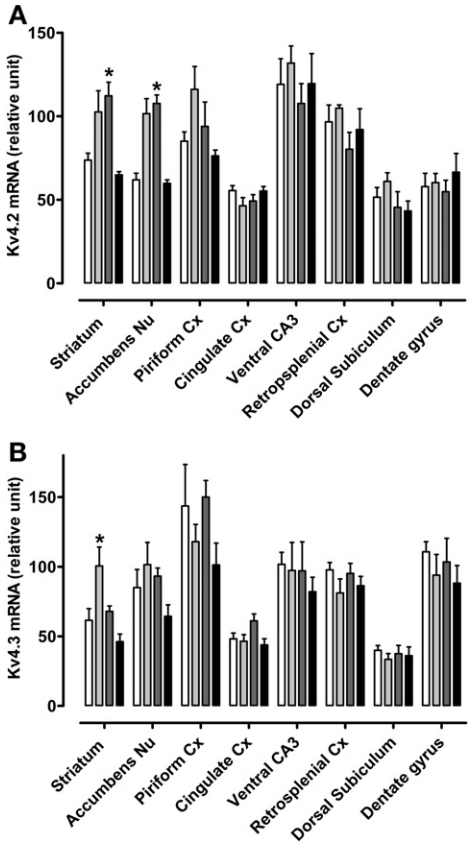

Figure 6. Kv4 mRNA temporal analysis. Kv4.2 (*A*) and Kv4.3 (*B*) mRNA levels for different structures in conditioned rats sacrificed 1 h after sessions 1 (white), 2 (light gray), 3 (dark gray), and 5 (black) (Kv4.2, $n = 5$; Kv4.3, $n = 5$). Data are expressed as mean ± SEM. (*) $P < 0.05$ in ANOVA for Kv4.2 mRNA session 3 compared to sessions 1 and 5, and for Kv4.3 mRNA session 2 compared to sessions 1 and 5.

spatial learning task for a given experimental group. All of the compared data were obtained from autoradiographs on the same film.

Across sessions, changes in the expression of Kv4.2 mRNA were observed in the striatum, nucleus accumbens (ANOVAs, $F_{(3,16)} \leq 6.49$, $P < 0.01$) (Fig. 6A). The expression of Kv4.2 mRNA 1 h after session 3 was significantly higher than after sessions 1 and 5 for the striatum (Scheffé, $P < 0.05$) and for the accumbens nucleus (Scheffé, $P < 0.05$). During the spatial learning task, Kv4.3 mRNA levels transiently varied in the striatum only ($F_{(3,16)} = 5.82$, $P < 0.01$) (Fig. 6B), with an increase 1 h after session 2 compared with sessions 1 and 5 (Scheffé, $P < 0.05$). No significant difference of Kv4.2 and Kv4.3 mRNA expression was found in the other structures that were analyzed (ANOVAs, $F_{(3,16)} \leq 2.96$, NS). In the pseudoconditioned group, expression of Kv4 mRNA did not vary during spatial learning (ANOVAs, $F_{(3.21)} \leq 1.81$, NS, data not shown).

Correlation between Kv4 mRNA expression and behavioral performance (Fig. 7)

To examine the relationship between behavior and Kv4 mRNA expression during the spatial learning task, a linear regression was performed at specific stages of learning. Particular attention was paid to the time points where there were statistical differences in Kv4 mRNA expression between the rat groups (i.e., 1 h after sessions 1 and 2).

At 1 h after session 1, linear regression showed that increased reference memory performance (i.e., decreases in reference memory error number) was significantly associated with increased Kv4.3 mRNA expression in the striatum, nucleus accumbens, and cingulate cortex ($F_{(1,4)} \geq 8.233$, $P < 0.05$). In contrast, no significant correlation was found between memory performance and Kv4.2 mRNA levels in any of the structures studied ($F_{(1.4)} \leq 1.623$, NS).

At 1 h following session 2, reference memory performance was positively correlated with Kv4.2 mRNA expression in the retrosplenial cortex only ($F_{(1,4)} = 12.430$, $P < 0.05$). In contrast, expression of Kv4.3 mRNA was not correlated with reference memory performance in any of the structures studied ($F_{(1.4)} \leq 5.765$, NS). No other significant correlations were seen for the other stages of learning for either Kv4 transcript (data not shown).

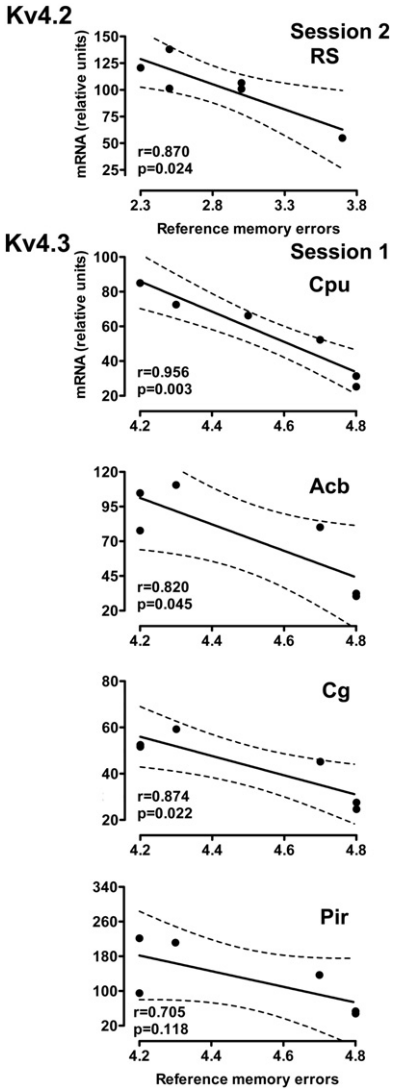

Figure 7. Relationships between learning performance and Kv4.2 and Kv4.3 subunit mRNA levels. Kv4.2 and Kv4.3 mRNA ISH labeling values were measured 1 h after session 2 (*top*) and 1 h after session 1 (*bottom*), respectively, for the conditioned group in different structures. Correlations between the levels of Kv4.2 and Kv4.3 subunit mRNAs and reference memory errors were identified by a simple linear regression analysis. (*) $P < 0.05$ is significant. Dotted lines correspond to the 95% confidence of regression line. (Acb) Nucleus accumbens; (Cg) cingulate cortex; (Cpu) caudate putamen; (Pir) piriform cortex; (RS) retrosplenial cortex.

Discussion

The blockade of AmmTX3-sensitive Kv4 channels impaired learning processes possibly through the combination of an increase in excitability and a reduction of GABAergic inhibition, leading to a strong reduction of input specificity. Thus, our results demonstrate that: (1) when injected during the early stages of learning, AmmTX3 delays consolidation of reference memory; (2) AmmTX3 increases and stabilizes the EPSP-spike potentiation induced in DG by a "weak" tetanus; (3) transcription of Kv4.2 and Kv4.3 is up-regulated in limbic-related structures only during the early stages of learning; (4) the level of expression of Kv4 mRNA is significantly correlated with learning.

AmmTX3 has been reported to contain two separate functional domains that block two different types of K+ channels: a low-affinity Ether-a-go-go-related (ERG) domain (Abdel-Mottaleb et al. 2008) and a high-affinity Kv4 domain. We therefore cannot exclude the possibility that AmmTX3 alters learning and memory processes by blocking ERG channels. However, there are no reports of involvement of ERG channels in learning and memory and LTP mechanisms. Moreover, only the Kv4 channel distribution completely overlaps with the AmmTX3 binding-site distribution. We therefore assume that all of our results concerning cognitive functioning are the consequence of Kv4 current inhibition.

AmmTX3 prolongs the E-S component of LTP

We performed the electrophysiological experiments in the dorsal DG because of its essential involvement in radial maze processing (McNaughton 1980; Sutherland et al. 1983; Jeltsch et al. 2001; Dumas et al. 2004; Niewoehner et al. 2007; Matsuo et al. 2009; Rubino et al. 2009). Our electrophysiological results are of three types.

First, IO curves and baseline recordings showed no effect of the toxin on basal synaptic transmission, as we observed no difference in EPSP slope or PS amplitude between groups under these conditions. Concerning the EPSP slope, the lack of such an effect is expected since there are probably very few Kv4.2 channels on glutamatergic synapses in DG, as suggested by studies on mice by Jinno et al. (2005). These investigators showed that these channels are clustered at postsynaptic sites of GABAergic-DG synapses. The findings for PS amplitude are more surprising, as blocking Kv4.2 and Kv4.3 channels had no effect on excitability during basal transmission. Because we used evoked field-potential recording, we cannot exclude an effect of the toxin on basal excitability of some neurons of the population recorded. However, it seems that the dose of the toxin (0.75 μg) was too low to elicit an increase of excitability of a significant part of this population under basal conditions, despite a relatively high level of Kv4 expression at baseline (Serôdio and Rudy 1998; Vacher et al. 2006). This dose has no effect on locomotor, feeding, or drinking activity, which is consistent with the absence of changes in excitability. We hypothesize that an up-regulation of Kv4 channels is the condition for such a low dose to be effective, either on E-S translation or on behavior, as discussed below (see paragraphs on long-term plasticity results and spatial learning performances). This lack of effect on basal transmission could be also due to the strong inhibition exerted by GABAergic interneurons observed in vivo in DG (Buckmaster and Schwartzkroin 1995), particularly when using a barbiturate anesthetic that enhances and prolongs inhibitory postsynaptic potential (Nicoll et al. 1975).

Second, we studied short-term plasticity using paired-pulse (PP) stimulations. We obtained similar levels of PP depression in both groups. This is consistent with a post-synaptic localization of Kv4.2 and Kv4.3 channels in the hippocampus (Jinno et al. 2005), assuming that this type of plasticity relies mainly on presynaptic changes. As an aside, the fact that we obtained only a depression whatever the interpulse delay used (10–160 msec) confirmed that we specifically stimulated the medial perforant path (MPP) (McNaughton 1980; Colino and Malenka 1993; Cho et al. 2007).

The final set of data was focused on long-term plasticity. Using HFS of the MPP, we induced E-S potentiation in Vehicle and AmmTX3 groups. In this type of LTP, the PS amplitude is increased for a given level of EPSP slope (Bliss and Lomo 1973). Indeed, while the EPSP slope returned to baseline after about 30 min post-induction, the PS amplitude remained potentiated for the whole 4 h of recording. These results are consistent with the kind of tetanus we used, which could be considered as "weak," as it consists of only two trains of HFS instead of the 10 trains normally used to obtain a "saturated" LTP (Jeffery and Morris 1993; Truchet et al. 2002). We chose such a weak HFS protocol to avoid a ceiling effect, which could have jeopardized our chances to observe a potential effect of the toxin. Besides, when using this type of tetanus in vivo in the DG, it is not unusual to observe dissociation between EPSP and PS levels (Kairiss et al. 1987).

Although the PS amplitude in the Vehicle group displayed a progressive decay following the tetanus, it remained stable in the AmmTX3 group during the entire 4 h of post-HFS recording; a delay of about 90 min seems necessary for the toxin to be effective on long-term plasticity, as the differences between the two groups became significant from this time point. We assume that this delay corresponds to the time needed to induce an up-regulation of Kv4 channels. Given that the toxin was injected intracerebroventricular (i.c.v.), one could only speculate on the mechanisms at play. A possibility could involve Ca^{2+}/calmodulin-dependent protein kinase II (CAMKII), since inhibiting this kinase leads to depotentiation within a similar time frame (Malinow et al. 1989). Indeed, E-S potentiation could induce an increase of CaMKII activity, as demonstrated in CA1 by Semyanov and Godukhin (2001), which in turn would up-regulate the expression of Kv4.2 channels. Moreover, Varga et al. (2004) showed that levels of Kv4.2 protein are increased with CaMKII phosphorylation in vitro. Thus, the effect of the toxin would climax thanks to this up-regulation, leading to the maintenance of E-S potentiation.

During an E-S potentiation, input specificity is strongly reduced, whether in vitro in CA1 (Jester et al. 1995) or in vivo in the DG (Abraham et al. 1985). Given the effect of AmmTX3 on E-S potentiation, we can therefore assume that in a behavioral context, AmmTX3 infusion could decrease the signal-to-noise ratio during information encoding.

In summary, our electrophysiological data show that AmmTX3 i.c.v. infusion prolongs and stabilizes the E-S component of LTP in the DG, with no effects on basal transmission or short-term plasticity. The reduction of input specificity associated with E-S potentiation is characterized by a decrease of the relative weight of the perforant path-DG synapses that are specifically activated by HFS. The reduction of the neuronal network specificity is consistent with the memory impairments observed in our behavioral studies.

Kv4 channel inhibition by AmmTX3 impairs reference memory and choice of learning strategy in a radial-maze task

Only a few studies have reported the behavioral effects of A-type current blockers. Kv4.2 knockout mice demonstrated an elevated stress response and an antidepressant resistance related to an increased neuronal excitability and an abnormal 5HT modulation (Lockridge et al. 2010). In a rat model of HIV-associated dementia, 4-aminopyridine (4-AP)—a broad spectrum A-type current inhibitor—restores impaired spatial memory (Keblesh et al. 2009). In

contrast to 4-AP, AmmTX3 did not alter the acquisition of information in our study, but instead impaired its consolidation. Indeed, the reference memory performances decreased when AmmTX3 was injected after session. This disruption persisted for at least 2 d after injection, and the spatial learning of the AmmTX3-treated group was delayed. The memory deficit induced by AmmTX3 treatment suggests that Kv4 channels modulate the consolidation of spatial learning.

Further analysis of reference memory data shows that the rats used an egocentric strategy at the start of training, i.e., they relied on their body position to guide their response by always turning right or left as they preferentially chose the neighbored arm for the next entry. In a radial-maze task, such a strategy is characterized by a high number of 45° turns (Klein et al. 2004). As training continues, this strategy is usually replaced by an allocentric one that requires memorization of a spatial map of the environment (representation of external cues) and involves very few 45° turns (Gal et al. 1997; Klein et al. 2004). In AmmTX3-treated rats, the number of 45° turns remained high, indicating that they used an egocentric strategy longer, whereas vehicle-treated rats quickly switched to a more appropriate allocentric strategy. This finding is consistent with a recent report showing a decreased use of spatial search strategies by Kv4.2 knockout mice (Lockridge and Yuan 2011). Our results therefore demonstrate the involvement of Kv4 channels in the consolidation of spatial information and learning strategy.

Spatial learning is related to transient Kv4 up-regulation

We analyzed the expression of Kv4.2 and Kv4.3 subunits at different stages of spatial learning through in situ hybridization of mRNAs. Expression of both Kv4 subunits increased during the early stages of spatial learning when the animals had not yet mastered the associations between rewarded arm location and spatial cues. At this learning stage, performance is strongly dependent on egocentric strategies (Schenk and Morris 1985; Gaytán-Tocavén and Olvera-Cortés 2004). The variations in Kv4 mRNA levels reflected pure learning processes, as no differences were detected between pseudoconditioned (exposed to the same stimuli and environment as conditioned rats) and naive rats remaining in the animal room.

In the hippocampus, expression of Kv4.2 channels was increased only in the ventral CA3 field, which is involved in the processing of stress and emotion but not in the dorsal hippocampus, which is involved in spatial memory (for review, see Fanselow and Dong 2010). Further investigations are necessary to understand the roles of the Kv4.2 subunits present in all of the Ammon's horn pyramidal neurons and of the Kv4.3 subunits mainly found in the CA3 field and hippocampal interneurons (Serôdio and Rudy 1998).

Up-regulation of Kv4 channels occurred in other structures of the limbic system, i.e., the retrosplenial cortex, dorsal subiculum, striatum, nucleus accumbens, and piriform cortices. All of these structures are involved in spatial memory and spatial navigation. Thus, retrosplenial lesions produce spatial deficits on tasks that rely on different spatial strategies. Furthermore, the retrosplenial cortex is intensively interconnected with the hippocampus and anterior thalamic nuclei, which are important for the switching between egocentric and allocentric strategies (Burgess et al. 2007; Burgess 2008; Aggleton 2009). The subiculum is in a pivotal position leading the output of the hippocampal formation. Indeed, subicular lesions in the rat do not affect a general navigational-directional strategy, but impair the integration of spatial information provided by extramaze cues in water maze tasks (Oswald and Good 2000; O'Mara et al. 2009). The dorsal striatum is known to be involved in the acquisition and expression of response learning by mediating egocentric behavior (Gold 2004; Packard 2009). In fact, during task acquisition the hippocampus and striatum operate in parallel, regardless of the cognitive strategy being used in multiple forms of learning (Yeshenko et al. 2004; Iglói et al. 2009; Jacobson et al. 2012). A competition between both systems occurs such that inactivation of one system may facilitate learning of the other strategy (Chang and Gold 2003; Lee et al. 2011; Moussa et al. 2011). The accumbens nucleus is also involved in spatial behavior and strategy selection. While a functional similarity between the dorsal striatum and accumbens nucleus is demonstrated in the processing of allocentric spatial information, a distinction between the two structures is found in the consolidation of egocentric spatial information (Klein et al. 2004; De Leonibus et al. 2005; Floresco et al. 2006; Haluk and Floresco 2009). Further investigations will be necessary to understand the functional implication of Kv4 channels in the mnesic process, for example, by studying the AmmTX3 infusion effects in these different structures during spatial learning tasks.

However, several studies reported a straight relation between A-type K+ currents and Kv4 channels in neostriatal neurons (Tkatch et al. 2000). Kv4 channels in the spiny neurons of the striatal medium regulate b-AP (Day et al. 2008) and participate in clustering and firing bursting patterns (Falk et al. 2006). In addition, these channels play an essential role in producing an A-type current in striatal cholinergic interneurons (Hattori et al. 2003). In these interneurons, Kv4 channels are consistent with their playing a role in governing the slow, repetitive discharge of interneurons in vivo (Song et al. 1998). Moreover, Kv4 channel activation could also be involved in the opioid modulation at corticostriatal synaptic terminals by the reduction of glutamate release (Jose et al. 2007). Then, Kv4 channel activation probably participates to modulation of synaptic signal transmission, shaping electrical signaling and synaptic plasticity that underlie mnesic processes.

So, the transient up-regulation of Kv4 channels associated with the negative effects of AmmTX3 on learning strategy and positive effect on E-S-potentiation suggests that Kv4 channels modulate cellular excitability in structures involved in strategy alternation during spatial learning.

What should be the consequences of increases of Kv4 subunit expression on mnesic processes? Changes in A-type Kv channel expression may modify excitability in the neuronal networks involved in spatial learning. The cellular and subcellular location of Kv4 mRNA was impossible to determine in our experiments. However, many reports indicate that Kv4.2 and Kv4.3 subunits are located in projection neurons and interneurons (Sheng et al. 1992; Martina et al. 1998; Serôdio and Rudy 1998; Rhodes et al. 2004; Jinno et al. 2005; Menegola et al. 2008). At this location, these channels are able to modulate neuronal excitability, as demonstrated in previous studies. The up-regulation of functional Kv4.2 channels will therefore lead to an increase in A-type K^+ current associated with modifications in NMDA subunit composition and a deficiency of LTP in hippocampal slice neurons (Jung et al. 2008). Conversely, when the expression of a Kv4.2 subunit is decreased in a dominant-negative model, the opposite effects are observed (Jung et al. 2008). Furthermore, the elimination of dendritic A-type K^+ currents in Kv4.2 knockdown mice enhances b-AP amplitude, increases neuronal excitability, and facilitates LTP induction in hippocampal neurons (Kim et al. 2005, 2007; Chen et al. 2006; Andrásfalvy et al. 2008; Zhao et al. 2011). Shen et al. (2008) have shown that enhancing excitatory input by glutamate in cortical neurons increases Kv4-channel-mediated K^+ current and, as a consequence, negatively regulated neuronal excitability. As neuronal excitability cooperates with synaptic transmission to control information storage (Shen et al. 2008), these findings along with our results are consistent with the

hypothesis that during spatial learning: (1) the increase of Kv4.3 mRNA levels is a sign of a reduction of the GABAergic influence, and (2) the increase of Kv4.2 mRNA levels contributes to a decrease of activity in the surrounding neurons of the learning-specific networks to assure a correct and specific storage of information. This coordinated balance of excitability may reinforce the signal-to-noise ratio associated with information encoding in the limbic and para-limbic structures during the early stages of learning.

In conclusion, we have demonstrated that Kv4 channels are an essential regulator of the excitability of specific networks that underlie spatial information learning, both inside and outside of the hippocampal formation. Further investigations are required to determine how Kv4-channel activity orchestrates the A-type potassium current modulation and affects the neuronal excitability changes involved in memory processes through spike timing-dependent plasticity. In particular, our next studies will focus on structures where we observed an up-regulation of Kv4 channel expression and on changes in this expression following LTP induction.

Materials and Methods

Animals and surgery

Male Sprague Dawley rats (280–400 g; Charles River Laboratories, Inc., France) were housed individually and supplied with food and water ad libitum. The animals were kept at a constant temperature under a 12-h light/12-h dark cycle. Before behavioral experiments, a cannula was implanted unilaterally in the lateral ventricle of rats anesthetized with ketamine (8 mg/100 g) (Imalgène 1000, Rhône-Mérieux) and xylazine (0.8 mg/100 g) (Rompun 2%, Bayer). The animals were allowed to recover for 7 d and were then handled for a maximum of 10 min per day on the 2 d before the behavioral experiment, regardless of the nature of the experiment. All experiments were carried out in accordance with the European Communities Council Directive (86/609/EEC). All efforts were made to minimize the numbers of animals used and to maintain them in good general health.

Drugs

AmmTX3 was generously donated by M.F. Martin-Eauclaire (CRN2M, CNRS–Université Aix-Marseille II, France). The recombinant AmmTX3 was produced in Escherichia coli as previously described (Abdel-Mottaleb et al. 2008). The method of Kourrich et al. (2001) was used to make an i.c.v. injection of 1.5 μL of AmmTX3 or vehicle (NaCl 0.9%).

Oligonucleotide probes

Oligodesoxynucleotide probes for the rat Kv4.2 subunit (44 bp) and Kv4.3 subunits (34 bp) were purchased and purified by reverse-phase chromatography from Eurogentec S.A. (France). The sense oligodesoxynucleotide was used as a negative control. The Kv4.2 antisense probe sequence was:

5′-CAGTGGCCACTTCCATGCAGCTTTCTTCAAAGACTTGTTCATCC-3′ (Pei et al. 1997). The position of the probe in referenced sequences is 1756-1712 (GenBank accession no. NM_031730). The sense probe sequence was: 5′-GTCACCGGTGAAGGTACGTCGAAAGAAGTTTCTGAACAAGTAGG-3′.

The Kv4.3 antisense probe sequence was:

5′-ACAAATGCCCCGGACACGTCCTCGTTGTTGGTCA-3′ (Serôdio et al. 1996). The position of this probe in referenced sequences is 918-885 (GenBank accession no. NM_031739). The sequence for the sense probe was: 5′-TGTTTACGGGGCCTGTGCAGGAGCAACAACCAGT-3′. Probe cDNA fragments were prepared by labeling the cDNA fragment with [^{35}S]dATP (1250 Ci/mmol) by the random primer method using a DNA-tailing kit and terminal deoxynucleotide transferase (Roche Diagnostics). The radiolabeled probes were then purified by gel-filtration chromatography and centrifugation (Quick Spin Columns, Roche). Radiolabeled probes were then stored at a specific activity (at least 1×10^6 cpm/μL) at 4°C.

Electrophysiology (see Supplemental Material for details)

Surgery

Intracerebral injection cannula (IIC, 26 ga.) was implanted unilaterally in the left ventricle. Stimulating and differential recording electrodes were placed ipsilateraly in the MPP and the DG, respectively.

Stimulating/recording protocol

After a fEPSP stabilization period, the protocol was: IO curves, PP stimulations, and 20-min baseline recording before and after AmmTX3/vehicle injection. After the second baseline, HFS were applied to the MPP, followed by 4 h of recording in DG.

Experimental parameters

HFS intensity was the same as for baseline and parameters were set to induce a moderate level of LTP. fEPSP slope and PS amplitude were normalized for each animal with respect to the mean values obtained during the baseline. Evoked responses were averaged in groups of four.

Spatial-learning task in eight-arm radial maze

The same spatial-learning task was used for both the AmmTX3 and ISH studies. The eight-arm radial maze was positioned in the center of the well-illuminated experimental room and several external visual cues were maintained in fixed locations throughout the experiment (Mpari et al. 2008). All rats were maintained at 85% of their ad libitum weight by food restriction and were subjected to two handling sessions (10 min) before testing began. Following a habituation period (Mpari et al. 2008), each animal received six training trials per day (one session) with a 2-min intertrial interval over a 5-d period. For each rat, a different pattern of three baited arms out of eight was chosen and extramaze cues remained the same throughout the experiment. Baits were placed in two adjacent arms and a third arm at 180° from one of the first two. The goal of the task was to retrieve all three food pellets. The rat was positioned in the center of the maze where all doors were closed for 15 sec before opening. Each training trial continued until all three baits had been consumed or until 7 min had elapsed. An arm entry was scored when all four paws of the rat were in the arm. Performance was assessed by three factors: reference memory errors (entry to an arm that was never baited) and working memory errors (repeat arm entries into any arm) and the number of total turn and of 45° rotations. The order of arm choices was also monitored.

For AmmTX3 studies, AmmTX3 was injected 30 min before session 2 or immediately after sessions 1, 3, or 5. Different groups of rats were used for each injection time. For ISH studies, pseudo-conditioned animals were trained as conditioned animals but the three baited arms were different in every training trial, thus excluding any possibility of establishing associations between arm-reward and extramaze spatial cues.

In situ hybridization procedures

Animals (vehicle $n = 6$, pseudoconditioned $n = 6$, and conditioned $n = 6$) were anesthetized with sodium pentobarbital (6%, Sanofi santé) and, depending on the group, decapitated at 1 h after the first, second, third, and fifth sessions. Brains were immediately removed, frozen, and stored at −80°C. Coronal (16-μm) thick tissue sections were taken at −20°C at the level of the cortices (frontal, piriform, dorsal cingulate, and retrosplenial), hippocampal formation (dorsal and ventral CA1, CA3, CA4 fields, dorsal

and ventral DG, dorsal and ventral subiculum), and basal ganglia (striatum [dorsal striatum], nucleus accumbens [ventral striatum]), median and lateral habenula, cerebellum (molecular and granular layers) based on the stereotaxic atlas of Paxinos and Watson (2007).

We performed two ISH experiments. In a first experiment (between-group analysis), brain sections from the three groups were collected for each brain region and for each time-point (i.e., 1 h after the first, second, third, and fifth sessions). These times were chosen because the AmmTX3 effect persisted on spatial reference memory during three sessions of our spatial task paradigm (see results section). To prevent experimental artifacts during analysis of the autoradiographs, sections were cut at the same brain level from naive and experimental groups of animals. Sections from the experimental groups at a particular learning stage were grouped together in the same ISH and exposed on the same autoradiographic film. In addition, sections of one naive rat used as an internal standard were added to all the ISH experiments to exclude possible experimental artifacts in the comparison of labeling in different learning stages. In a second experiment (within-group temporal analysis), we collected brain sections from rats sacrificed at four different time points for each brain level and for each group (i.e., vehicle, pseudoconditioned, and conditioned rats). Both experiments were conducted using identical ISH protocols.

In situ hybridization

Slide-mounted sections were post-fixed for 5 min in 4% paraformaldehyde and were rinsed in a phosphate vehicle buffer (PBS). The sections were then acetylated for 10 min with 0.25% acetic anhydride in 0.1 M triethanolamine, dehydrated, and air dried.

Each section was covered with labeled probe (5×10^5 cpm/section) diluted in 35 μL of hybridization solution (50% formamide, 10% dextran sulfate, 1X Denhardt's solution, 1% yeast tRNA, 1% sheared salmon sperm DNA, 4X SSC) and incubated in humid chambers for 12 h at 42°C or 45°C, respectively, for the Kv4.2 or Kv4.3 probe.

After hybridization, the sections were washed sequentially in 1X SSC for 30 min at room temperature, 1X SSC for 30 min (55°C for Kv4.2 probe, 45°C Kv4.3 probe), 1X SSC 30 min, and 0.1X SSC at room temperature.

The hybridization signal was detected by autoradiography using Kodak Bio-Max MR-1 film for 20 d.

Data analysis

Behavioral and electrophysiological tasks

Statistical analysis was performed with the SPSS/PC statistics 11 software package (SPSS, Inc.). The following behavioral variables were analyzed during training: the number of reference memory and working memory errors, the total number of turns after the first arm visit. The data were analyzed by multivariate analysis of variance (MANOVA) with repeated measures. Selected ANOVA was then performed, followed by two-tailed Scheffé's post hoc tests. Electrophysiological data were analyzed with two-way ANOVA. Statistical significance was a P value < 0.05.

The response-strategy criterion has been previously defined (Gal et al. 1997; Mpari et al. 2008). A statistical analysis of the turning response strategy was performed using a normal approximation to the binomial distribution with $P = 2/7$ and $n = 24$. The number of turns was determined when a rat performed six trials without error in two sessions before the injection (two turning responses × six trials × two sessions). The 0° turning response (re-entering the arm) was not analyzed and the turning direction (clockwise or counter-clockwise) was not considered.

In situ hybridization experiments

Autoradiographs were analyzed through quantification of radioactivity with NIH Image software. ^{14}C plastic standards (Amersham) were used to calibrate the concentration of ^{35}S. Mean density was calculated for each nucleus, using six to eight bilateral measurements in each animal. The group-value presented for each structure studied is the mean of the values obtained for each animal ± SEM.

Acknowledgments

This research was supported by the Centre National de la Recherche Scientifique and by the Aix-Marseille Université. We thank Valérie Demare, Valérie Gilbert, and Elodie Mansour for technical support. We also thank Dr. Marie-France Martin-Eauclaire, Dr. Hélène Vacher, and Dr. Bruno Poucet for critical reading of this manuscript.

References

Abdel-Mottaleb Y, Corzo G, Martin-Eauclaire M-F, Satake H, Céard B, Peigneur S, Nambaru P, Bougis P-E, Possani LD, Tytgat J. 2008. A common "hot spot" confers hERG blockade activity to α-scorpion toxins affecting K+ channels. *Biochem Pharmacol* **76:** 805–815.

Abraham WC, Bliss TV, Goddard GV. 1985. Heterosynaptic changes accompany long-term but not short-term potentiation of the perforant path in the anaesthetized rat. *J Physiol (Lond)* **363:** 335–349.

Abraham WC, Gustafsson B, Wigström H. 1987. Long-term potentiation involves enhanced synaptic excitation relative to synaptic inhibition in guinea-pig hippocampus. *J Physiol (Lond)* **394:** 367–380.

Aggleton JP. 2009. Understanding retrosplenial amnesia: Insights from animal studies. *Neuropsychologia* **48:** 2328–2338.

Andrásfalvy BK, Makara JK, Johnston D, Magee JC. 2008. Altered synaptic and non-synaptic properties of CA1 pyramidal neurons in Kv4.2 knockout mice. *J Physiol (Lond)* **586:** 3881–3892.

Birnbaum SG, Varga AW, Yuan L-L, Anderson AE, Sweatt JD, Schrader LA. 2004. Structure and function of Kv4-family transient potassium channels. *Physiol Rev* **84:** 803–833.

Bliss TV, Lomo T. 1973. Long-lasting potentiation of synaptic transmission in the dentate area of the anaesthetized rabbit following stimulation of the perforant path. *J Physiol (Lond)* **232:** 331–356.

Buckmaster PS, Schwartzkroin PA. 1995. Interneurons and inhibition in the dentate gyrus of the rat in vivo. *J Neurosci* **15:** 774–789.

Burgess N. 2008. Spatial cognition and the brain. *Ann N Y Acad Sci* **1124:** 77–97.

Burgess N, Barry C, O'Keefe J. 2007. An oscillatory interference model of grid cell firing. *Hippocampus* **17:** 801–812.

Chang Q, Gold PE. 2003. Switching memory systems during learning: Changes in patterns of brain acetylcholine release in the hippocampus and striatum in rats. *J Neurosci* **23:** 3001–3005.

Chen X, Yuan L-L, Zhao C, Birnbaum SG, Frick A, Jung WE, Schwarz TL, Sweatt JD, Johnston D. 2006. Deletion of Kv4.2 gene eliminates dendritic A-type K^+ current and enhances induction of long-term potentiation in hippocampal CA1 pyramidal neurons. *J Neurosci* **26:** 12143–12151.

Cho MH, Cao X, Wang D, Tsien JZ. 2007. Dentate gyrus-specific manipulation of β-Ca2+/calmodulin-dependent kinase II disrupts memory consolidation. *Proc Natl Acad Sci* **104:** 16317–16322.

Colino A, Malenka RC. 1993. Mechanisms underlying induction of long-term potentiation in rat medial and lateral perforant paths in vitro. *J Neurophysiol* **69:** 1150–1159.

Day M, Wokosin D, Plotkin JL, Tian X, Surmeier DJ. 2008. Differential excitability and modulation of striatal medium spiny neuron dendrites. *J Neurosci* **28:** 11603–11614.

De Leonibus E, Oliverio A, Mele A. 2005. A study on the role of the dorsal striatum and the nucleus accumbens in allocentric and egocentric spatial memory consolidation. *Learn Mem* **12:** 491–503.

Dumas TC, Powers EC, Tarapore PE, Sapolsky RM. 2004. Overexpression of calbindin D(28k) in dentate gyrus granule cells alters mossy fiber presynaptic function and impairs hippocampal-dependent memory. *Hippocampus* **14:** 701–709.

Falk T, Zhang S, Erbe EL, Sherman SJ. 2006. Neurochemical and electrophysiological characteristics of rat striatal neurons in primary culture. *J Comp Neurol* **494:** 275–289.

Fanselow MS, Dong H-W. 2010. Are the dorsal and ventral hippocampus functionally distinct structures? *Neuron* **65:** 7–19.

Floresco SB, Ghods-Sharifi S, Vexelman C, Magyar O. 2006. Dissociable roles for the nucleus accumbens core and shell in regulating set shifting. *J Neurosci* **26:** 2449–2457.

Gal G, Joel D, Gusak O, Feldon J, Weiner I. 1997. The effects of electrolytic lesion to the shell subterritory of the nucleus accumbens on delayed non-matching-to-sample and four-arm baited eight-arm radial-maze tasks. *Behav Neurosci* **111:** 92–103.

Gaytán-Tocavén L, Olvera-Cortés ME. 2004. Bilateral lesion of the cerebellar-dentate nucleus impairs egocentric sequential learning but not egocentric navigation in the rat. *Neurobiol Learn Mem* **82:** 120–127.

Gold PE. 2004. Coordination of multiple memory systems. *Neurobiol Learn Mem* **82:** 230–242.

Haluk DM, Floresco SB. 2009. Ventral striatal dopamine modulation of different forms of behavioral flexibility. *Neuropsychopharmacology* **34:** 2041–2052.

Hammond RS, Lin L, Sidorov MS, Wikenheiser AM, Hoffman DA. 2008. Protein kinase a mediates activity-dependent Kv4.2 channel trafficking. *J Neurosci* **28:** 7513–7519.

Hattori S, Murakami F, Song W-J. 2003. Quantitative relationship between Kv4.2 mRNA and A-type K^+ current in rat striatal cholinergic interneurons during development. *J Neurophysiol* **90:** 175–183.

Iglói K, Zaoui M, Berthoz A, Rondi-Reig L. 2009. Sequential egocentric strategy is acquired as early as allocentric strategy: Parallel acquisition of these two navigation strategies. *Hippocampus* **19:** 1199–1211.

Jacobson TK, Gruenbaum BF, Markus EJ. 2012. Extensive training and hippocampus or striatum lesions: Effect on place and response strategies. *Physiol Behav* **105:** 645–652.

Jeffery KJ, Morris RG. 1993. Cumulative long-term potentiation in the rat dentate gyrus correlates with, but does not modify, performance in the water maze. *Hippocampus* **3:** 133–140.

Jeltsch H, Bertrand F, Lazarus C, Cassel JC. 2001. Cognitive performances and locomotor activity following dentate granule cell damage in rats: Role of lesion extent and type of memory tested. *Neurobiol Learn Mem* **76:** 81–105.

Jester JM, Campbell LW, Sejnowski TJ. 1995. Associative EPSP—spike potentiation induced by pairing orthodromic and antidromic stimulation in rat hippocampal slices. *J Physiol (Lond)* **484:** 689–705.

Jinno S, Jeromin A, Kosaka T. 2005. Postsynaptic and extrasynaptic localization of Kv4.2 channels in the mouse hippocampal region, with special reference to targeted clustering at gabaergic synapses. *Neuroscience* **134:** 483–494.

Jo A, Kim HK. 2011. Up-regulation of dendritic Kv4.2 mRNA by activation of the NMDA receptor. *Neurosci Lett* **496:** 129–134.

Jose X, Pineda JC, Rodriguez C, Mendoza E, Galarraga E, Bargas J, Barral J. 2007. δ opioids reduce the neurotransmitter release probability by enhancing transient (K_V4) K^+-currents in corticostriatal synapses as evaluated by the paired pulse protocol. *Neurosci Lett* **414:** 150–154.

Jung S-C, Kim J, Hoffman DA. 2008. Rapid, bidirectional remodeling of synaptic NMDA receptor subunit composition by A-type K^+ channel activity in hippocampal CA1 pyramidal neurons. *Neuron* **60:** 657–671.

Kairiss EW, Abraham WC, Bilkey DK, Goddard GV. 1987. Field potential evidence for long-term potentiation of feed-forward inhibition in the rat dentate gyrus. *Brain Res* **401:** 87–94.

Keblesh JP, Dou H, Gendelman HE, Xiong H. 2009. 4-Aminopyridine improves spatial memory in a murine model of HIV-1 encephalitis. *J Neuroimmune Pharmacol* **4:** 317–327.

Kim J, Hoffman DA. 2008. Potassium channels: Newly found players in synaptic plasticity. *Neuroscientist* **14:** 276–286.

Kim J, Wei D-S, Hoffman DA. 2005. Kv4 potassium channel subunits control action potential repolarization and frequency-dependent broadening in rat hippocampal CA1 pyramidal neurones. *J Physiol (Lond)* **569:** 41–57.

Kim J, Jung S-C, Clemens AM, Petralia RS, Hoffman DA. 2007. Regulation of dendritic excitability by activity-dependent trafficking of the A-type K^+ channel subunit Kv4.2 in hippocampal neurons. *Neuron* **54:** 933–947.

Klein S, Hadamitzky M, Koch M, Schwabe K. 2004. Role of glutamate receptors in nucleus accumbens core and shell in spatial behaviour of rats. *Neuroscience* **128:** 229–238.

Kourrich S, Mourre C, Soumireu-Mourat B. 2001. Kaliotoxin, a Kv1.1 and Kv1.3 channel blocker, improves associative learning in rats. *Behav Brain Res* **120:** 35–46.

Lauver A, Yuan L-L, Jeromin A, Nadin BM, Rodríguez JJ, Davies HA, Stewart MG, Wu G-Y, Pfaffinger PJ. 2006. Manipulating Kv4.2 identifies a specific component of hippocampal pyramidal neuron A-current that depends upon Kv4.2 expression. *J Neurochem* **99:** 1207–1223.

Lee HY, Ge W-P, Huang W, He Y, Wang GX, Rowson-Baldwin A, Smith SJ, Jan YN, Jan LY. 2011. Bidirectional regulation of dendritic voltage-gated potassium channels by the fragile × mental retardation protein. *Neuron* **72:** 630–642.

Lei Z, Deng P, Li Y, Xu ZC. 2010. Downregulation of Kv4.2 channels mediated by NR2B-containing NMDA receptors in cultured hippocampal neurons. *Neuroscience* **165:** 350–362.

Lockridge A, Yuan L-L. 2011. Spatial learning deficits in mice lacking A-type K^+ channel subunits. *Hippocampus* **21:** 1152–1156.

Lockridge A, Su J, Yuan LL. 2010. Abnormal 5-HT modulation of stress behaviors in the Kv4.2 knockout mouse. *Neuroscience* **170:** 1086–1097.

Lugo JN, Barnwell LF, Ren Y, Lee WL, Johnston LD, Kim R, Hrachovy RA, Sweatt JD, Anderson AE. 2008. Altered phosphorylation and localization of the A-type channel, Kv4.2 in status epilepticus. *J Neurochem* **106:** 1929–1940.

Magee JC, Johnston D. 1997. A synaptically controlled, associative signal for Hebbian plasticity in hippocampal neurons. *Science* **275:** 209–213.

Magee JC, Johnston D. 2005. Plasticity of dendritic function. *Curr Opin Neurobiol* **15:** 334–342.

Maletic-Savatic M, Lenn NJ, Trimmer JS. 1995. Differential spatiotemporal expression of K+ channel polypeptides in rat hippocampal neurons developing in situ and in vitro. *J Neurosci* **15:** 3840–3851.

Malinow R, Schulman H, Tsien RW. 1989. Inhibition of postsynaptic PKC or CaMKII blocks induction but not expression of LTP. *Science* **245:** 862–866.

Martina M, Schultz JH, Ehmke H, Monyer H, Jonas P. 1998. Functional and molecular differences between voltage-gated K^+ channels of fast-spiking interneurons and pyramidal neurons of rat hippocampus. *J Neurosci* **18:** 8111–8125.

Matsuo N, Yamasaki N, Ohira K, Takao K, Toyama K, Eguchi M, Yamaguchi S, Miyakawa T. 2009. Neural activity changes underlying the working memory deficit in α-CaMKII heterozygous knockout mice. *Front Behav Neurosci* **3:** 20. doi: 10.3389/neuro.08.020.2009.

McNaughton BL. 1980. Evidence for two physiologically distinct perforant pathways to the fascia dentata. *Brain Res* **199:** 1–19.

Menegola M, Trimmer JS. 2006. Unanticipated region- and cell-specific downregulation of individual KChIP auxiliary subunit isotypes in Kv4.2 knock-out mouse brain. *J Neurosci* **26:** 12137–12142.

Menegola M, Misonou H, Vacher H, Trimmer JS. 2008. Dendritic A-type potassium channel subunit expression in CA1 hippocampal interneurons. *Neuroscience* **154:** 953–964.

Monaghan MM, Menegola M, Vacher H, Rhodes KJ, Trimmer JS. 2008. Altered expression and localization of hippocampal A-type potassium channel subunits in the pilocarpine-induced model of temporal lobe epilepsy. *Neuroscience* **156:** 550–562.

Morozov A, Muzzio IA, Bourtchouladze R, Van-Strien N, Lapidus K, Yin D, Winder DG, Adams JP, Sweatt JD, Kandel ER. 2003. Rap1 couples cAMP signaling to a distinct pool of p42/44MAPK regulating excitability, synaptic plasticity, learning, and memory. *Neuron* **39:** 309–325.

Moussa R, Poucet B, Amalric M, Sargolini F. 2011. Contributions of dorsal striatal subregions to spatial alternation behavior. *Learn Mem* **18:** 444–451.

Mpari B, Sreng L, Regaya I, Mourre C. 2008. Small-conductance Ca^{2+}-activated K^+ channels: Heterogeneous affinity in rat brain structures and cognitive modulation by specific blockers. *Eur J Pharmacol* **589:** 140–148.

Nicoll RA, Eccles JC, Oshima T, Rubia F. 1975. Prolongation of hippocampal inhibitory postsynaptic potentials by barbiturates. *Nature* **258:** 625–627.

Niewoehner B, Single FN, Hvalby Ø, Jensen V, Meyer zum Alten Borgloh S, Seeburg PH, Rawlins JNP, Sprengel R, Bannerman DM. 2007. Impaired spatial working memory but spared spatial reference memory following functional loss of NMDA receptors in the dentate gyrus. *Eur J Neurosci* **25:** 837–846.

O'Mara SM, Sanchez-Vives MV, Brotons-Mas JR, O'Hare E. 2009. Roles for the subiculum in spatial information processing, memory, motivation and the temporal control of behaviour. *Prog Neuropsychopharmacol Biol Psychiatry* **33:** 782–790.

Oswald CJ, Good M. 2000. The effects of combined lesions of the subicular complex and the entorhinal cortex on two forms of spatial navigation in the water maze. *Behav Neurosci* **114:** 211–217.

Packard MG. 2009. Exhumed from thought: Basal ganglia and response learning in the plus-maze. *Behav Brain Res* **199:** 24–31.

Paxinos G, Watson C. 2007. *The rat brain in stereotaxic coordinates*. Academic Press, Amsterdam, The Netherlands.

Pei Q, Burnet PW, Grahame-Smith DG, Zetterström TS. 1997. Differential effects of acute and chronic electroconvulsive shock on the abundance of messenger RNAs for voltage-dependent potassium channel subunits in the rat brain. *Neuroscience* **78:** 343–350.

Pisciotta M, Coronas FI, Bloch C, Prestipino G, Possani LD. 2000. Fast K^+ currents from cerebellum granular cells are completely blocked by a peptide purified from *Androctonus australis* Garzoni scorpion venom. *Biochim Biophys Acta* **1468:** 203–212.

Ramakers GMJ, Storm JF. 2002. A postsynaptic transient K^+ current modulated by arachidonic acid regulates synaptic integration and threshold for LTP induction in hippocampal pyramidal cells. *Proc Natl Acad Sci* **99:** 10144–10149.

Rhodes KJ, Carroll KI, Sung MA, Doliveira LC, Monaghan MM, Burke SL, Strassle BW, Buchwalder L, Menegola M, Cao J, et al. 2004. KChIPs and Kv4 α subunits as integral components of A-type potassium channels in mammalian brain. *J Neurosci* **24:** 7903–7915.

Rubino T, Realini N, Braida D, Guidi S, Capurro V, Viganò D, Guidali C, Pinter M, Sala M, Bartesaghi R, et al. 2009. Changes in hippocampal morphology and neuroplasticity induced by adolescent THC treatment are associated with cognitive impairment in adulthood. *Hippocampus* **19:** 763–772.

Schenk F, Morris RG. 1985. Dissociation between components of spatial memory in rats after recovery from the effects of retrohippocampal lesions. *Exp Brain Res* **58:** 11–28.

Semyanov A, Godukhin O. 2001. Epileptiform activity and EPSP-spike potentiation induced in rat hippocampal CA1 slices by repeated high-K^+: Involvement of ionotropic glutamate receptors and Ca^{2+}/calmodulin-dependent protein kinase II. *Neuropharmacology* **40:** 203–211.

Serôdio P, Rudy B. 1998. Differential expression of Kv4 K^+ channel subunits mediating subthreshold transient K^+ (A-type) currents in rat brain. *J Neurophysiol* **79:** 1081–1091.

Serôdio P, Vega-Saenz de Miera E, Rudy B. 1996. Cloning of a novel component of A-type K^+ channels operating at subthreshold potentials with unique expression in heart and brain. *J Neurophysiol* **75:** 2174–2179.

Shen B, Zhou K, Yang S, Xu T, Wang Y. 2008. The Kv4.2 mediates excitatory activity-dependent regulation of neuronal excitability in rat cortical neurons. *J Neurochem* **105:** 773–783.

Sheng M, Tsaur ML, Jan YN, Jan LY. 1992. Subcellular segregation of two A-type K^+ channel proteins in rat central neurons. *Neuron* **9:** 271–284.

Song WJ, Tkatch T, Baranauskas G, Ichinohe N, Kitai ST, Surmeier DJ. 1998. Somatodendritic depolarization-activated potassium currents in rat neostriatal cholinergic interneurons are predominantly of the A type and attributable to coexpression of Kv4.2 and Kv4.1 subunits. *J Neurosci* **18:** 3124–3137.

Sutherland RJ, Whishaw IQ, Kolb B. 1983. A behavioural analysis of spatial localization following electrolytic, kainate- or colchicine-induced damage to the hippocampal formation in the rat. *Behav Brain Res* **7:** 133–153.

Tkatch T, Baranauskas G, Surmeier DJ. 2000. Kv4.2 mRNA abundance and A-type K^+ current amplitude are linearly related in basal ganglia and basal forebrain neurons. *J Neurosci* **20:** 579–588.

Truchet B, Chaillan FA, Soumireu-Mourat B, Roman FS. 2002. Learning and memory of cue-reward association meaning by modifications of synaptic efficacy in dentate gyrus and piriform cortex. *Hippocampus* **12:** 600–608.

Tsaur ML, Chou CC, Shih YH, Wang HL. 1997. Cloning, expression and CNS distribution of Kv4.3, an A-type K^+ channel α subunit. *FEBS Lett* **400:** 215–220.

Vacher H, Romi-Lebrun R, Mourre C, Lebrun B, Kourrich S, Masméjean F, Nakajima T, Legros C, Crest M, Bougis PE, et al. 2001. A new class of scorpion toxin binding sites related to an A-type K^+ channel: Pharmacological characterization and localization in rat brain. *FEBS Lett* **501:** 31–36.

Vacher H, Alami M, Crest M, Possani LD, Bougis PE, Martin-Eauclaire M-F. 2002. Expanding the scorpion toxin α-KTX 15 family with AmmTX3 from *Androctonus mauretanicus*. *Eur J Biochem* **269:** 6037–6041.

Vacher H, Prestipino G, Crest M, Martin-Eauclaire MF. 2004. Definition of the α-KTx15 subfamily. *Toxicon* **43:** 887–894.

Vacher H, Diochot S, Bougis PE, Martin-Eauclaire M-F, Mourre C. 2006. Kv4 channels sensitive to BmTX3 in rat nervous system: Autoradiographic analysis of their distribution during brain ontogenesis. *Eur J Neurosci* **24:** 1325–1340.

Varga AW, Anderson AE, Adams JP, Vogel H, Sweatt JD. 2000. Input-specific immunolocalization of differentially phosphorylated Kv4.2 in the mouse brain. *Learn Mem* **7:** 321–332.

Varga AW, Yuan L-L, Anderson AE, Schrader LA, Wu G-Y, Gatchel JR, Johnston D, Sweatt JD. 2004. Calcium-calmodulin-dependent kinase II modulates Kv4.2 channel expression and upregulates neuronal A-type potassium currents. *J Neurosci* **24:** 3643–3654.

Watanabe S, Hoffman DA, Migliore M, Johnston D. 2002. Dendritic K^+ channels contribute to spike-timing dependent long-term potentiation in hippocampal pyramidal neurons. *Proc Natl Acad Sci* **99:** 8366–8371.

Yeshenko O, Guazzelli A, Mizumori SJY. 2004. Context-dependent reorganization of spatial and movement representations by simultaneously recorded hippocampal and striatal neurons during performance of allocentric and egocentric tasks. *Behav Neurosci* **118:** 751–769.

Yuan L-L, Adams JP, Swank M, Sweatt JD, Johnston D. 2002. Protein kinase modulation of dendritic K^+ channels in hippocampus involves a mitogen-activated protein kinase pathway. *J Neurosci* **22:** 4860–4868.

Zhao C, Wang L, Netoff T, Yuan L-L. 2011. Dendritic mechanisms controlling the threshold and timing requirement of synaptic plasticity. *Hippocampus* **21:** 288–297.

Received December 22, 2011; accepted in revised form April 27, 2012.